Hollow Spheres

Deutsche Ausgabe: DOI: 10.1002/ange.201608410
Internationale Ausgabe: DOI: 10.1002/anie.201608410

Formation of Triple-Shelled Molybdenum–Polydopamine Hollow Spheres and Their Conversion into MoO_2/Carbon Composite Hollow Spheres for Lithium-Ion Batteries

*Yawen Wang[+], Le Yu[+], and Xiong Wen (David) Lou**

Abstract: *Unique triple-shelled Mo-polydopamine (Mo-PDA) hollow spheres are synthesized through a facile solvothermal process. A sequential self-templating mechanism for the multi-shell formation is proposed, and the number of shells can be adjusted by tuning the size of the Mo-glycerate templates. These triple-shelled Mo-PDA hollow spheres can be converted to triple-shelled MoO_2/carbon composite hollow spheres by thermal treatment. Owing to the unique multi-shells and hollow interior, the as-prepared MoO_2/carbon composite hollow spheres exhibit appealing performance as an anode material for lithium-ion batteries, delivering a high capacity of ca. 580 mAh g^{-1} at 0.5 A g^{-1} with good rate capability and long cycle life.*

Designed synthesis of nanostructures has always been one of the major research focuses in the development of nanotechnology. Among all the innovative nanostructures, a large number of multi-shelled hollow structures with different compositions and structures have been developed in recent years.[1,2] Compared to normal single-shelled hollow particles, which have the advantage of the large void volume and high surface-to-volume ratio,[2–4] it is believed that multi-shelled hollow structures can gain extra benefits from the inner structures.[1,2,5] Specifically, the complex inner structures could improve volumetric energy density and power density by increasing the weight fraction of active species, and also prolong the cycle life due to the enhanced structural stability.[1,6]

Although multi-shelled hollow structures are expected to exhibit better performance for some applications for example as electrode materials for lithium-ion batteries, it would be increasingly difficult to synthesize multi-shelled hollow particles as compared to the synthesis of single- or double-shelled hollow structures. Common strategies include hard-templating methods, soft-templating methods and some template-free self-assembly methods.[1] Hard-templating methods employ some sacrificial templates to facilitate the shell material growth. Early attempts of synthesizing multi-shelled nanostructures using this method usually require repeated deposition of interlayer and precursors, making the whole process rather tedious.[7] Nevertheless, there are some multi-shelled nanostructures reported, for example, multiple-shelled SiO_2[8] and Au@SiO_2[9] hollow particles have been reported by repetitive SiO_2 deposition. Recently, Wang et al. developed a general method using carbonaceous microspheres as the template to synthesize multi-shelled metal oxide hollow spheres.[10] With careful control of the reaction parameters, multi-shelled α-Fe_2O_3, Co_3O_4, NiO, CuO, ZnO, and $ZnFe_2O_4$ hollow spheres are successfully prepared by a sequential templating growth method.[11] Soft-templating methods on the other hand use self-assembled micelles or vesicles as templates.[12–14] Though such soft templates are easy to remove, it is usually quite challenging to control the reaction system involving soft templates. Template-free methods have not yet been thoroughly explored as they are usually based on some unusual mechanisms with only few reported examples such as the self-assembled multi-shelled azithromycin hollow microspheres.[15]

Molybdenum dioxide (MoO_2) has been suggested as a promising anode material for lithium-ion batteries (LIBs) owing to its relatively high electrical conductivity, high reversible capacity (838 mAh g^{-1}), and good chemical stability.[16] Recently, a number of nanostructured MoO_2 and MoO_2-based nanocomposites, including MoO_2 nanoparticles,[17] nanosheets,[18] nanorods,[19] nanotubes,[20] yolk–shell nanospheres[21] and hollow microspheres,[22,23] as well as MoO_2/carbon hybrids like MoO_2/graphene composites,[24–26] MoO_2/C core–shell spheres,[27] MoO_2/C hollow spheres,[28,29] carbon-coated MoO_2 nanobelts,[30] etc., have been reported with enhanced electrochemical performance for LIBs. In particular, MoO_2/C hollow spheres have been prepared by precipitating MoO_2 on the polyvinylpyrrolidone (PVP) soft template.[29]

Herein we report a facile synthesis of triple-shelled Mo-polydopamine (Mo-PDA) hollow spheres by a solvothermal process. Utilizing previously reported Mo-glycerate (MoG) spheres as the precursor,[31] Mo-PDA hollow spheres with triple-shells are successfully synthesized by reacting the MoG spheres with dopamine hydrochloride in a mixed ethanol/H_2O solvent at elevated temperature. The formation mechanism of the triple-shelled hollow structures is investigated in detail, and a sequential self-templating mechanism is deduced. Furthermore, the important role of ammonia in this system is studied. By adjusting the amount of ammonia added and the size of the initial MoG solid spheres, the number of shells in Mo-PDA hollow spheres could be adjusted from one to four. The triple-shelled Mo-PDA

[*] Dr. Y. Wang,[+] Dr. L. Yu,[+] Prof. X. W. Lou
School of Chemical and Biomedical Engineering
Nanyang Technological University
62 Nanyang Drive, Singapore 637459 (Singapore)
E-mail: xwlou@ntu.edu.sg
davidlou88@gmail.com
Homepage: http://www.ntu.edu.sg/home/xwlou/
[+] These authors contributed equally to this work.

Supporting information for this article can be found under: http://dx.doi.org/10.1002/anie.201608410.

hollow spheres are further annealed to form MoO_2/C composite hollow spheres which are shown to exhibit enhanced electrochemical performance as an anode material for LIBs.

The synthesis process of the triple-shelled Mo-PDA hollow spheres is schematically illustrated in Figure 1 a. First, MoG solid spheres with a diameter of ca. 790 nm (Figure S1, Supporting Information (SI)) are synthesized by a previously reported method with slight modifications.[31,32] In the next step, the obtained MoG solid spheres react with dopamine hydrochloride in the presence of ammonia at 140 °C. Under such alkaline condition, dopamine polymerizes at the surface of MoG spheres while the MoG solid spheres are slowly etched. The simultaneous dissolution and polymerization processes lead to the formation of the triple-shelled Mo-PDA hollow structures.

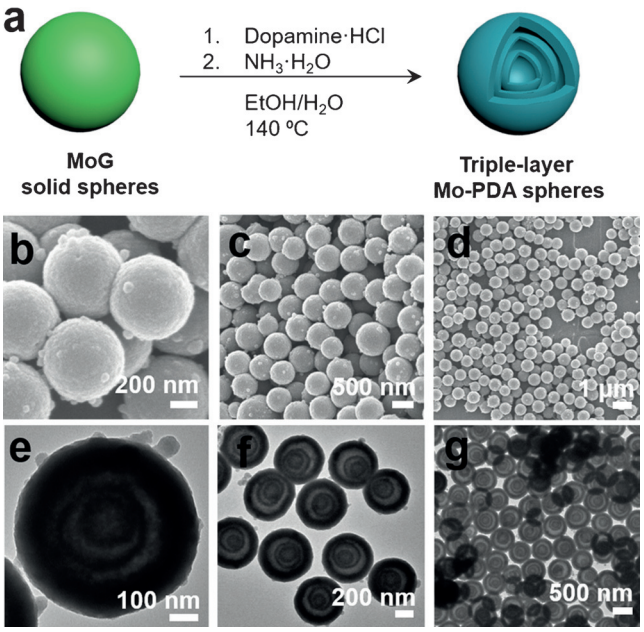

Figure 1. a) Illustration of the synthesis process, b–d) FESEM and e–g) TEM images of the as-synthesized triple-shelled Mo-PDA hollow spheres.

The morphology and internal structure of the as-synthesized triple-shelled Mo-PDA hollow spheres are shown in Figure 1 b–g. From the field-emission scanning electron microscope (FESEM) and transmission electron microscopy (TEM) images, it can be found that the Mo-PDA hollow spheres are quite uniform, and possess very smooth surface over the whole particle without any crystalline facets. The average diameters of three shells are 650 nm, 350 nm and 190 nm. The outermost shell is thicker than the less spherical inner shells. The Mo-PDA hollow spheres are generally smaller than the initial MoG solid spheres, perhaps because the polymerization process becomes significant only after the initiation of the MoG dissolution process. Energy-dispersive X-ray (EDX) spectroscopy data of the Mo-PDA hollow spheres confirms the existence of the elements of Mo, C and O (Figure S2, SI). The X-ray diffraction (XRD) pattern of the triple-shelled hollow spheres shows multiple peaks below 30° belonging to an unknown phase, which is likely Mo-polydopamine,[33] while the XRD pattern of the precursor MoG spheres exhibits only broad peaks (Figure S3, SI). Thermogravimetric analysis (TGA; Figure S4, SI) also shows that, compared to the MoG solid spheres, the weight loss of the Mo-PDA hollow spheres increases from 15 % to about 65 %, indicating the presence of a higher content of carbonaceous material in the Mo-PDA hollow spheres. Fourier transform infrared (FTIR) spectra of different samples (MoG solid spheres, triple-shelled Mo-PDA hollow spheres and polydopamine particles) indicate the existence of polydopamine in the Mo-PDA hollow spheres (Figure S5, SI).

The formation mechanism of the triple-shelled Mo-PDA hollow spheres is then investigated in detail. Simply heating the MoG solid spheres in the presence of ammonia would cause etching of the MoG spheres, and the product looks like collapsed structures (Figure S6a, SI). On the other hand, without the MoG solid spheres, the dopamine polymerization still takes place and yields small polydopamine nanoparticles with irregular shapes (Figure S6b, SI). Thus it can be concluded that two processes, the dissolution of the MoG solid spheres and the polymerization of dopamine, take place simultaneously during the solvothermal process.

The transformation from MoG solid spheres to Mo-PDA hollow spheres is found to be very fast. While the particles after reaction for 40 min (Figure S7a, SI) are still solid, the product after reaction for 50 min contains almost all triple-shelled hollow spheres (Figure S7b, SI). From the sample obtained at 45 min, different intermediate particles can be observed (Figure S7c,d, SI). From these observations, a sequential self-templating mechanism can be deduced (Figure 2 a). The alkaline-catalyzed polymerization should have started as soon as the addition of $NH_3·H_2O$. However, due to the low concentration of $NH_3·H_2O$, it proceeds at

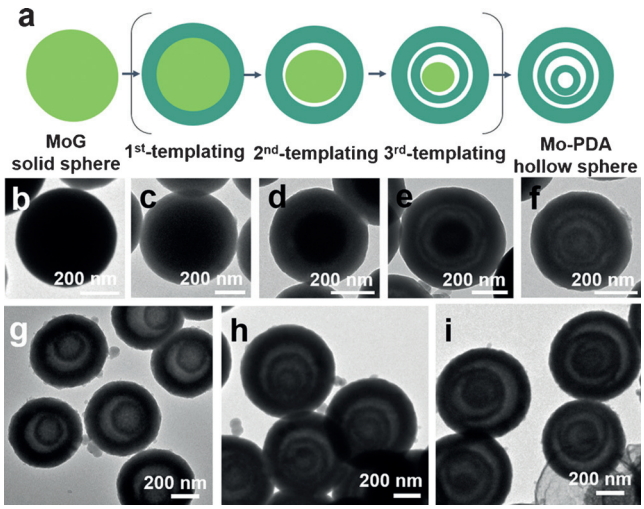

Figure 2. a) Formation of triple-shelled Mo-PDA hollow spheres by the sequential self-templating mechanism; b–f) TEM images of the intermediates captured during the transformation process; g–i) double-shelled (g), triple-shelled (h) and quadruple-shelled (i) Mo-PDA hollow spheres formed by using MoG spheres with diameters of 580 nm, 830 nm and 1100 nm, respectively.

a relatively low rate at room temperature (Figure 2b). Only after the temperature rises, the first-stage templated growth process takes place while MoG particles have already been etched from the surface. The TEM image of the intermediate shows clear core–shell structure as the outer shell has a lighter contrast (Figure 2c). The next two intermediates include the one with a yolk–shell structure which has a gap between the internal solid core and the outer shell, and the other with a yolk–shell structure containing two outer shells (Figure 2d,e), suggesting the templating growth happens in a sequential manner. And finally, the inner-most solid core is etched to form the triple-shelled hollow spheres (Figure 2f).

The structure of the multi-shelled Mo-PDA hollow spheres can be controlled by adjusting the size of the MoG solid spheres. When smaller MoG spheres (ca. 580 nm in diameter; Figure S8a, SI) are used, double-shelled hollow spheres are obtained instead of triple-shelled structures (Figure 2g). On the other hand, triple-shelled hollow spheres with a size of ca. 720 nm (Figure 2h) are still formed when the size of the MoG spheres is about 830 nm (Figure S8b, SI). When the size of the MoG spheres is further increased to 1100 nm (Figure S8c, SI), the large template particles even allow the formation of another shell and give rise to some quadruple-shelled hollow spheres (Figure 2i). This relationship between the number of shells and the size of the MoG templates further supports the proposed sequential self-templating mechanism.

The amount of ammonia ($NH_3{\cdot}H_2O$) is another important parameter in the reaction system that greatly affects the rate of the dopamine polymerization (Figure S9a, SI). In literature, polymerization of dopamine is normally carried out at room temperature.[33,34] The chemical process of dopamine polymerization should have started at room temperature. But in the present case due to the low concentration of ammonia (10 μL), the rate of polymerization would only become significant as the temperature rises during which the dissolution process of the MoG spheres always takes place. When a much higher amount of ammonia is used (40 μL), almost all hollow spheres obtained are single-shelled (Figure S9b, SI). This is because such excess amount of ammonia would greatly accelerate the polymerization of dopamine, leading to quick depletion of the monomers during the temperature rising period. If most of the dopamine monomers are consumed before the start of MoG dissolution, there would be no dopamine monomers left for the later templated growth processes which construct the inner structures. On the other hand, deficient amount of ammonia (5 μL) induces slow polymerization of dopamine, which can only lead to formation of mesoporous inner structures (Figure S9d, SI). Only when moderate amount of ammonia (20 μL) is added, multi-shelled hollow structures can be formed (Figure S9c, SI).

The as-prepared triple-shelled Mo-PDA hollow spheres are further annealed in N_2 atmosphere at 600 °C for 6 h to obtain triple-shelled MoO_2/C hollow spheres. The panoramic FESEM images (Figure 3a,b) show that the overall spherical morphology is well preserved. Compared to the Mo-PDA hollow spheres, the size of these MoO_2/C hollow spheres shrinks to ca. 500 nm. TEM images (Figure 3c,d) further reveal the inner shells, well-defined gaps and inner-most cavities by the sharp contrast between shells and the voids. EDX analysis confirms the existence of Mo, C, and O in the annealed product (Figure 3e). XRD study of the triple-shelled hollow spheres (Figure 3f) shows relatively weak peaks that can be indexed to the tugarinovite MoO_2 phase (JCPDS card no. 32-0671). TGA analysis shows that the content of MoO_2 is about 27 wt% in the MoO_2/C composite hollow spheres (Figure S4, SI). Raman spectrum demonstrates that the graphitization degree of the MoO_2/C sample is relatively low (Figure S10, SI). As determined by N_2 sorption measurement (Figure S11, SI), the triple-shelled hollow spheres possess a Brunauer–Emmett–Teller (BET) specific surface area of 60.9 $m^2 g^{-1}$.

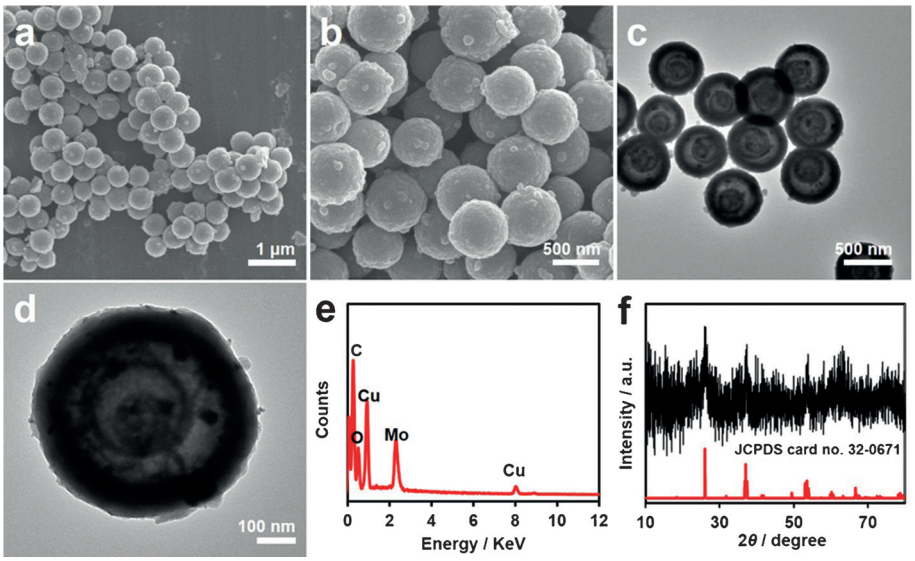

Figure 3. a,b) FESEM and c,d) TEM images of triple-shelled MoO_2/C composite hollow spheres obtained by annealing the triple-shelled Mo-PDA hollow spheres at 600 °C at 5 °C min^{-1} for 6 h in N_2 atmosphere. e) EDX and f) XRD patterns of the triple-shelled MoO_2/C composite hollow spheres.

The triple-shelled MoO_2/C hollow spheres are evaluated as an anode material for LIBs. Figure 4a shows the representative galvanostatic charge/discharge voltage profiles in the voltage range of 0.01–3.0 V versus Li/Li^+ at a current density of 0.5 A g^{-1}. A voltage plateau located at 0.8 V can be observed in the first discharge, corresponding to the formation of Li_xMoO_2 by the insertion of Li^+ ions into the MoO_2 lattice. As lithium storage in MoO_2 follows the conversion reaction type of mechanism, there are generally no well-defined voltage plateaus during the subsequent charging/

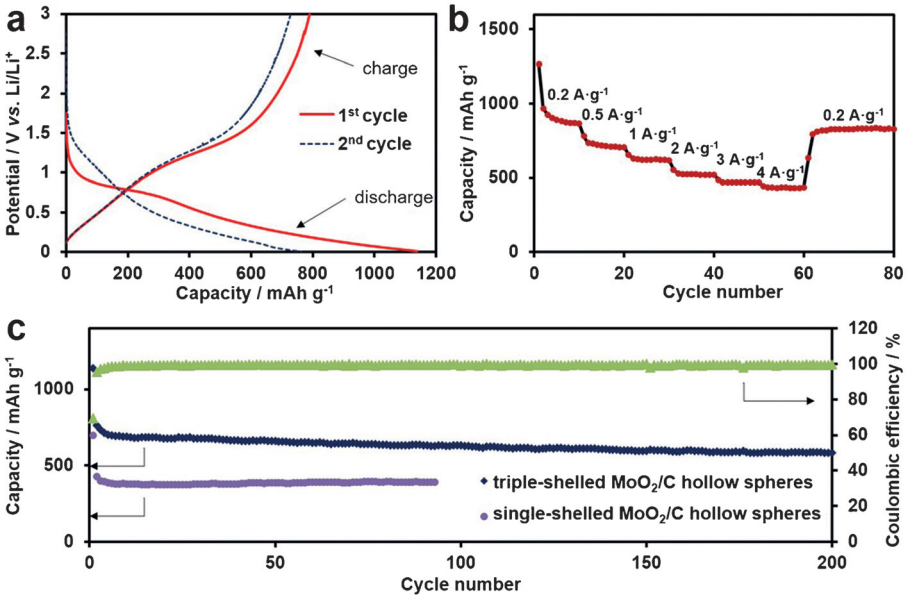

Figure 4. a) Charge–discharge voltage profiles at 0.5 $A g^{-1}$ and b) rate capability of the triple-shelled MoO_2/C hollow spheres. c) Cycling performance and Coulombic efficiency of triple-shelled MoO_2/C hollow spheres at 0.5 $A g^{-1}$. The cycling performance of single-shelled MoO_2/C hollow spheres is also provided in (c) for comparison at the same current density.

discharging processes. The discharge capacity of the triple-shelled MoO_2/C hollow spheres in the first cycle is 1139 $mAh g^{-1}$ with a Coulombic efficiency of 67% due to irreversible processes such as the formation of the solid–electrolyte interface (SEI) film and decomposition of electrolyte.[35,36] Cyclic voltammetry (CV) measurements of the triple-shelled MoO_2/C hollow spheres (Figure S12, SI) also indicate the typical lithiation/delithiation process of MoO_2. Galvanostatic charging–discharging measurements confirm that these unique triple-shelled MoO_2/C hollow spheres can be reversibly cycled at various current densities. As shown in Figure 4b, the average specific capacities of the MoO_2/C hollow spheres are about 867, 709, 618, 529, 469 and 433 $mAh g^{-1}$ at the current densities of 0.2, 0.5, 1, 2, 3 and 4 $A g^{-1}$, respectively. When the current density is reduced back to 0.2 $A g^{-1}$, a high capacity of 825 $mAh g^{-1}$ is immediately resumed, suggesting the good reversibility of the electrode materials. The cycling performance of the triple-shelled MoO_2/C hollow spheres electrodes is presented in Figure 4c. The triple-shelled MoO_2/C hollow spheres deliver a reversible specific capacity of about 580 $mAh g^{-1}$ at 0.5 $A g^{-1}$ after 200 cycles. Importantly, the Coulombic efficiency is nearly 100% after the first few cycles. It should be noted that both MoO_2 and carbon components contribute to the measured specific capacity. But it is not easy to determine exactly the relative contribution of each component to the total specific capacity as it is very hard to selectively remove MoO_2 even in strong acidic solution (Figure S13, SI). Moreover, this performance is superior to that of many other MoO_2/carbon composites (Table S1, SI). From Figure 4c, it is also interesting to note that the single-shelled MoO_2/C hollow spheres (Figure S14, SI) exhibit much lower specific capacities although the cycling is also quite stable. The higher capacity of the multi-shelled hollow spheres might be related to the increment of electrochemical active sites compared to the single-shelled hollow spheres with a much lower BET specific surface area of 29.7 $m^2 g^{-1}$ (Figure S15, SI). The double-shelled and quadruple-shelled Mo-PDA hollow spheres can also be converted to corresponding MoO_2/C composite hollow spheres with reduced quality for the quadruple-shelled sample and generally lower specific capacities (Figure S16, SI).

In summary, triple-shelled Mo-polydopamine hollow spheres have been synthesized by simply reacting preformed uniform Mo-glycerate solid spheres with dopamine under alkaline condition via a solvothermal process. An interesting sequential self-templating mechanism is revealed to account for the formation of triple-shelled hollow spheres. After thermal treatment in inert atmosphere, the Mo-polydopamine hollow spheres are transformed into MoO_2/carbon composite hollow spheres. When evaluated as an electrode material for lithium-ion batteries, these triple-shelled MoO_2/carbon hollow spheres exhibit excellent electrochemical performance with high specific capacities and excellent cycling stability.

Acknowledgements

X.W.L. acknowledges funding support from the Ministry of Education of Singapore through Academic Research Fund (AcRF) Tier-1 Funding (M4011154.120; RG12/13).

Keywords: hollow spheres · lithium-ion batteries · MoO_2 · triple-shelled spheres

How to cite: *Angew. Chem. Int. Ed.* **2016**, *55*, 14668–14672
Angew. Chem. **2016**, *128*, 14888–14892

[1] J. Qi, X. Lai, J. Wang, H. Tang, H. Ren, Y. Yang, Q. Jin, L. Zhang, R. Yu, G. Ma, Z. Su, H. Zhao, D. Wang, *Chem. Soc. Rev.* **2015**, *44*, 6749–6773.
[2] X. Lai, J. E. Halpert, D. Wang, *Energy Environ. Sci.* **2012**, *5*, 5604–5618.
[3] Z. Wang, L. Zhou, X. W. Lou, *Adv. Mater.* **2012**, *24*, 1903–1911.
[4] X. Wang, J. Feng, Y. Bai, Q. Zhang, Y. Yin, *Chem. Rev.* **2016**, *116*, 10983–11060.
[5] Y. Li, J. Shi, *Adv. Mater.* **2014**, *26*, 3176–3205.
[6] X. Y. Yu, L. Yu, X. W. Lou, *Adv. Energy Mater.* **2016**, *6*, 1501333.
[7] F. Caruso, R. A. Caruso, H. Möhwald, *Science* **1998**, *282*, 1111–1114.
[8] C.-C. Huang, W. Huang, C.-S. Yeh, *Biomaterials* **2011**, *32*, 556–564.

[9] Y. J. Wong, L. Zhu, W. S. Teo, Y. W. Tan, Y. Yang, C. Wang, H. Chen, *J. Am. Chem. Soc.* **2011**, *133*, 11422 – 11425.
[10] Z. Li, X. Lai, H. Wang, D. Mao, C. Xing, D. Wang, *J. Phys. Chem. C* **2009**, *113*, 2792 – 2797.
[11] X. Lai, J. Li, B. A. Korgel, Z. Dong, Z. Li, F. Su, J. Du, D. Wang, *Angew. Chem. Int. Ed.* **2011**, *50*, 2738 – 2741; *Angew. Chem.* **2011**, *123*, 2790 – 2793.
[12] H. Xu, W. Wang, *Angew. Chem. Int. Ed.* **2007**, *46*, 1489 – 1492; *Angew. Chem.* **2007**, *119*, 1511 – 1514.
[13] J. Liu, S. B. Hartono, Y. G. Jin, Z. Li, G. Q. Lu, S. Z. Qiao, *J. Mater. Chem.* **2010**, *20*, 4595 – 4601.
[14] D. Gu, H. Bongard, Y. Deng, D. Feng, Z. Wu, Y. Fang, J. Mao, B. Tu, F. Schüth, D. Zhao, *Adv. Mater.* **2010**, *22*, 833 – 837.
[15] H. Zhao, J.-F. Chen, Y. Zhao, L. Jiang, J.-W. Sun, J. Yun, *Adv. Mater.* **2008**, *20*, 3682 – 3686.
[16] X. Hu, W. Zhang, X. Liu, Y. Mei, Y. Huang, *Chem. Soc. Rev.* **2015**, *44*, 2376 – 2404.
[17] J. H. Ku, J. H. Ryu, S. H. Kim, O. H. Han, S. M. Oh, *Adv. Funct. Mater.* **2012**, *22*, 3658 – 3664.
[18] H. Zhang, L. Zeng, X. Wu, L. Lian, M. Wei, *J. Alloys Compd.* **2013**, *580*, 358 – 362.
[19] B. Guo, X. Fang, B. Li, Y. Shi, C. Ouyang, Y.-S. Hu, Z. Wang, G. D. Stucky, L. Chen, *Chem. Mater.* **2012**, *24*, 457 – 463.
[20] H.-J. Zhang, J. Shu, K.-X. Wang, X.-T. Chen, Y.-M. Jiang, X. Wei, J.-S. Chen, *J. Mater. Chem. A* **2014**, *2*, 80 – 86.
[21] X. Zhang, X. Song, S. Gao, Y. Xu, X. Cheng, H. Zhao, L. Huo, *J. Mater. Chem. A* **2013**, *1*, 6858 – 6864.
[22] H. Zhang, Y. Li, Z. Hong, M. Wei, *Mater. Lett.* **2012**, *79*, 148 – 151.
[23] W. Pan, X. Liu, X. Miao, J. Yang, J. Wang, Y. Nuli, S.-i. Hirano, *J. Solid State Electrochem.* **2015**, *19*, 3347 – 3353.
[24] Y. Sun, X. Hu, W. Luo, Y. Huang, *ACS Nano* **2011**, *5*, 7100 – 7107.
[25] F. Xia, X. Hu, Y. Sun, W. Luo, Y. Huang, *Nanoscale* **2012**, *4*, 4707 – 4711.
[26] K. H. Seng, G. D. Du, L. Li, Z. X. Chen, H. K. Liu, Z. P. Guo, *J. Mater. Chem.* **2012**, *22*, 16072 – 16077.
[27] J. Besnardiere, X. Petrissans, C. Surcin, V. Buissette, T. Le Mercier, M. Morcrette, D. Portehault, S. Cassaignon, *RSC Adv.* **2014**, *4*, 21208 – 21215.
[28] H. Gao, C.-L. Liu, Y. Liu, Z.-H. Liu, W.-S. Dong, *Mater. Chem. Phys.* **2014**, *147*, 218 – 224.
[29] X. Liu, D. Wu, W. Ji, W. Hou, *J. Mater. Chem. A* **2015**, *3*, 968 – 972.
[30] L. Yang, L. Liu, Y. Zhu, X. Wang, Y. Wu, *J. Mater. Chem.* **2012**, *22*, 13148 – 13152.
[31] Y. Wang, L. Yu, X. W. Lou, *Angew. Chem. Int. Ed.* **2016**, *55*, 7423 – 7426; *Angew. Chem.* **2016**, *128*, 7549 – 7552.
[32] L. Shen, L. Yu, H. B. Wu, X.-Y. Yu, X. Zhang, X. W. Lou, *Nat. Commun.* **2015**, *6*, 6694.
[33] F.-X. Ma, H. B. Wu, B. Y. Xia, C.-Y. Xu, X. W. Lou, *Angew. Chem. Int. Ed.* **2015**, *54*, 15395 – 15399; *Angew. Chem.* **2015**, *127*, 15615 – 15619.
[34] A. Postma, Y. Yan, Y. Wang, A. N. Zelikin, E. Tjipto, F. Caruso, *Chem. Mater.* **2009**, *21*, 3042 – 3044.
[35] H. Hwang, H. Kim, J. Cho, *Nano Lett.* **2011**, *11*, 4826 – 4830.
[36] J. Zhou, J. Qin, X. Zhang, C. Shi, E. Liu, J. Li, N. Zhao, C. He, *ACS Nano* **2015**, *9*, 3837 – 3848.

Received: August 28, 2016
Revised: October 6, 2016
Published online: October 24, 2016

